

Lattice Codes for CRYSTALS-Kyber

Shuiyin Liu, *Member, IEEE*, Amin Sakzad, *Member, IEEE*

Abstract—This letter describes a lattice encoder for the NIST-recommended post-quantum encryption algorithm: Kyber. The key idea is to refine the analysis of Kyber decoding noise. We prove that Kyber decoding noise can be bounded by a sphere. This result shows the Kyber encoding problem is essentially a sphere packing in a hypercube. Lattice codes are then constructed to ensure denser packing and a lower decryption failure rate (DFR). Compared with the original Kyber encoder, the communication cost is reduced by up to 32.6%, the DFR is reduced by a factor of up to 2^{85} . The security arguments remain the same.

I. INTRODUCTION

The currently deployed Internet key exchange protocols use RSA and Elliptic Curve-based public-key cryptography (ECC), which have been proven to be vulnerable to quantum computing attacks. In July 2022, the National Institute of Standards and Technology (NIST) announced that a new post-quantum algorithm, Kyber, will replace current RSA and ECC-based key-establishment algorithms [1]. The NIST draft standard for Kyber was released in August 2023 [2]. However, the quantum resistance of Kyber is achieved at high communication cost, which refers to the ciphertext expansion rate (CER), i.e., the ratio of the ciphertext size to the plaintext size. Kyber introduces a 24–49 times more communication cost compared to ECC-based algorithms, which limits its practical application for resource-constrained devices.

Kyber uses the module learning with errors problem (MLWE) as its underlying mathematical problem [3]. Some recent research models the decryption decoding problem in LWE-based encryption schemes as the decoding problem on additive white Gaussian noise (AWGN) channels [4] [5]. Coding theory is then applied to improve the performance of LWE-based approaches. In [4], rate-1/2 polar codes were applied to Kyber, to reduce the decryption failure rate (DFR). In [5], Barnes–Wall lattice codes were used in FrodoKEM, to reduce the ciphertext size. However, the decoding noise in Kyber contains a large uniform component: Kyber uses a compression function to round the 12-bit ciphertext coefficients to 4-bit (KYBER512/768) or 5-bit (KYBER1024) integers. When decompressed, a 7 or 8-bit (almost) uniform noise will be added to the ciphertext [6]. For Kyber decoding, the assumption on the AWGN channel may not hold true.

In this work, we will demonstrate how to reduce the DFR and communication cost of Kyber. The main contribution of this paper is twofold: first, we show that the Kyber encoding problem is equivalent to the sphere packing in a hypercube. An

explicit tail bound on the decoding noise magnitude is derived. This result allows us to upper bound the Kyber decoding noise as a hypersphere. Second, we propose a lattice-based encoder for Kyber, to ensure the densest packing of the noise sphere. Note that the original Kyber encoder uses a scaled integer lattice, which is far from optimal. Our construction is based on Barnes–Wall lattice and Leech lattice since they are denser than the integer lattice and have fixed-complexity optimal decoders. Compared with the original Kyber encoder, the proposed lattice encoder reduces the CER by up to 32.6%, and improves the DFR by a factor of up to 2^{85} .

II. SYSTEM MODEL

A. Notation

Rings: Let R and R_q denote the rings $\mathbb{Z}[X]/(X^n + 1)$ and $\mathbb{Z}_q[X]/(X^n + 1)$, respectively. The degree n of the monic polynomial is fixed to 256 in Kyber. Matrices and vectors are represented as bold upper-case and lower-case letters, respectively. We use \mathbf{v}^T to represent the transpose of \mathbf{v} .

Sampling and Distribution: For a set S , we write $s \leftarrow S$ to denote that s is chosen uniformly at random from S . If S is a probability distribution, then this denotes that s is chosen according to the distribution S . For a polynomial $f(x) \in R_q$ or a vector of such polynomials, this notation is defined coefficient-wise. We use $\text{Var}(S)$ to represent the variance of the distribution S . Let x be a bit string and S be a distribution taking x as the input, then $y \sim S := \text{Sam}(x)$ represents that the output y generated by distribution S and input x can be extended to any desired length. We denote $\beta_\eta = B(2\eta, 0.5) - \eta$ as the central binomial distribution over \mathbb{Z} .

Compress and Decompress: Let $x \in \mathbb{R}$ be a real number, then $\lceil x \rceil$ means rounding to the closet integer with ties rounded up. Let $x \in \mathbb{Z}_q$ and $d \in \mathbb{Z}$ be such that $2^d < q$. We define

$$\begin{aligned} \text{Compress}_q(x, d) &= \lceil (2^d/q) \cdot x \rceil \pmod{2^d}, \\ \text{Decompress}_q(x, d) &= \lceil (q/2^d) \cdot x \rceil. \end{aligned} \quad (1)$$

B. Kyber: Key Generation, Encryption, and Decryption

Let k, d_u, d_v be positive integer parameters, which are listed in Table I. Let $\mathcal{M}_{2,n} = \{0, 1\}^n$ denote the message space, where every message $m \in \mathcal{M}_{2,n}$ can be viewed as a polynomial in R with coefficients in $\{0, 1\}$. Consider the public-key encryption scheme $\text{Kyber.CPA} = (\text{KeyGen}; \text{Enc}; \text{Dec})$ as described in Algorithms 1 to 3 [6].

Algorithm 1 $\text{Kyber.CPA.KeyGen}()$: key generation

- 1: $\rho, \sigma \leftarrow \{0, 1\}^{256}$
 - 2: $\mathbf{A} \sim R_q^{k \times k} := \text{Sam}(\rho)$
 - 3: $(\mathbf{s}, \mathbf{e}) \sim \beta_{\eta_1}^k \times \beta_{\eta_1}^k := \text{Sam}(\sigma)$
 - 4: $\mathbf{t} := \mathbf{A}\mathbf{s} + \mathbf{e}$
 - 5: **return** $(pk := (\mathbf{t}, \rho), sk := \mathbf{s})$
-

S. Liu is with the Cyber Security Research and Innovation Centre, Holmes Institute, Melbourne, VIC 3000, Australia (e-mail: SLiu@Holmes.edu.au). A. Sakzad is with the Department of Software Systems & Cybersecurity, Monash University, Melbourne VIC 3180, Australia (e-mail: Amin.Sakzad@monash.edu).

Algorithm 2 Kyber.CPA.Enc ($pk = (\mathbf{t}, \rho), m \in \mathcal{M}_{2, n}$)

```

1:  $r \leftarrow \{0, 1\}^{256}$ 
2:  $\mathbf{A} \sim R_q^{k \times k} := \text{Sam}(\rho)$ 
3:  $(\mathbf{r}, \mathbf{e}_1, e_2) \sim \beta_{\eta_1}^k \times \beta_{\eta_2}^k \times \beta_{\eta_2} := \text{Sam}(r)$ 
4:  $\mathbf{u} := \text{Compress}_q(\mathbf{A}^T \mathbf{r} + \mathbf{e}_1, d_u)$ 
5:  $v := \text{Compress}_q(\mathbf{t}^T \mathbf{r} + e_2 + \lceil q/2 \rceil \cdot m, d_v)$ 
6: return  $c := (\mathbf{u}, v)$ 

```

Algorithm 3 Kyber.CPA.Dec($sk = \mathbf{s}, c = (\mathbf{u}, v)$)

```

1:  $\mathbf{u} := \text{Decompress}_q(\mathbf{u}, d_u)$ 
2:  $v := \text{Decompress}_q(v, d_v)$ 
3: return  $\text{Compress}_q(v - \mathbf{s}^T \mathbf{u}, 1)$ 

```

TABLE I
KYBER PARAMETERS IN [2] [6]: PLAINTEXT SIZE: 256 BITS

	k	q	η_1	η_2	d_u	d_v	δ	CER
KYBER512	2	3329	3	2	10	4	2^{-139}	24
KYBER768	3	3329	2	2	10	4	2^{-164}	34
KYBER1024	4	3329	2	2	11	5	2^{-174}	49

C. Kyber Decoding Noise

Let n_e be the decoding noise in Kyber. According to [6] [4], we can write n_e as

$$n_e = v - \mathbf{s}^T \mathbf{u} - \lceil q/2 \rceil \cdot m \\ = \mathbf{e}^T \mathbf{r} + e_2 + c_v - \mathbf{s}^T (\mathbf{e}_1 + \mathbf{c}_u), \quad (2)$$

where $c_v \leftarrow \psi_{d_v}$, $\mathbf{c}_u \leftarrow \psi_{d_u}^k$ are rounding-off noises generated due to the compression operation. The elements in c_v or \mathbf{c}_u are assumed to be i.i.d. and independent of other terms in (2). For a small d , e.g., $d = d_v$, we can assume that ψ_d follows a discrete uniform distribution [3]:

$$c_v \leftarrow \psi_{d_v} \approx \mathcal{U}(-\lceil q/2^{d_v+1} \rceil, \lceil q/2^{d_v+1} \rceil). \quad (3)$$

Kyber decoding problem can thus be formulated as

$$y = \lceil q/2 \rceil \cdot m + n_e, \quad (4)$$

i.e., given the observation $y \in R_q$, recover the value of m .

From a coding perspective, an interesting question is if we can model (4) as an AWGN channel. Given the values of q and d_v in Table I, we observe that n_e contains a uniform component c_v with relatively large variance: 3640 for KYBER512 and KYBER768, and 918.67 for KYBER1024. Therefore, n_e may not follow a normal distribution and hence (4) may not be treated as an AWGN channel.

In Fig. 1, we compare the distribution of first coefficient in n_e , denoted as $n_{e,1}$, with the normal distribution using MATLAB function `normplot()`. If the sample data has a normal distribution, then the data points appear along the reference line. With 100,000 samples, we observe that the distribution of $n_{e,1}$ is different from the normal distribution. This result confirms that the AWGN assumption (4) of [4] is not valid.

D. Decryption Failure Rate and Ciphertext Expansion Rate

We let $\text{DFR} \triangleq \Pr(\hat{m} \neq m)$. Since the original Kyber encodes and decodes m bit-by-bit, DFR can be calculated by [3]:

$$\text{DFR} = \delta := \Pr(\|n_e\|_\infty \geq \lceil q/4 \rceil). \quad (5)$$

Note that it is desirable to have a small δ , e.g., $\delta < 2^{-128}$, in order to be safe against decryption failure attacks. In this work, the communication cost refers to the ciphertext expansion rate (CER), i.e., the ratio of the ciphertext size to the plaintext size. The values of δ and CER are given in Table I.

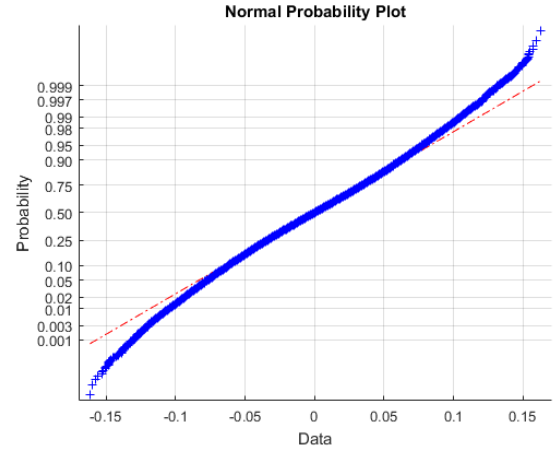


Fig. 1. KYBER768: Comparing the distribution of $n_{e,1}$ to the normal distribution with 100,000 samples.

III. THE ANALYSIS ON n_e

A. The Distribution of n_e

Theorem 1: According to the Central Limit Theorem (CLT), the distribution of n_e asymptotically approaches the sum of multivariate normal and uniform random variables:

$$n_e \leftarrow \mathcal{N}(0, \sigma_G^2 I_n) + \mathcal{U}(-\lceil q/2^{d_v+1} \rceil, \lceil q/2^{d_v+1} \rceil), \quad (6)$$

where $\sigma_G^2 = kn\eta_1^2/4 + kn\eta_1/2 \cdot (\eta_2/2 + \text{Var}(\psi_{d_u})) + \eta_2/2$. The values of $\text{Var}(\psi_{d_u})$ are listed in Table II.

Proof: See Appendix A. ■

The following lemma is used to prove Theorem 1.

Lemma 1: Suppose that $Z \leftarrow \beta_\eta$ and $Z' \leftarrow \beta_{\eta'}$, then the polynomial product ZZ' (modulo $X^n + 1$) asymptotically approaches a multivariate normal distribution for large n , i.e.,

$$ZZ' \leftarrow \mathcal{N}(0, n/4 \cdot \eta\eta' I_n).$$

Proof: See Appendix B. ■

Remark 1: The idea of Theorem 1 and Lemma 1 is to approximate a discrete normal distribution by a continuous normal distribution. This approximation is commonly used in LWE literature [5] [6]. The result in Lemma 1 can be easily generalised to the polynomial product of normal and binomial distributions, and two normal distributions as shown in [7].

In Table II, we show the CLT-based noise analysis for Kyber. We consider the normalised noise term $n_e / \lceil q/2 \rceil$ and evaluate its variance. The values of $\text{Var}(\psi_{d_u})$ are computed numerically as explained in [6]. We see that the estimated normalised variances match the simulation results.

TABLE II
KYBER DECODING NOISE VARIANCE (NORMALIZED)

	$\text{Var}(\psi_{d_u})$	CLT	Simulation	# of samples
KYBER512	0.9 [6]	0.0023	0.0023	10,000
KYBER768	0.9 [6]	0.0021	0.0021 [4]	10,000
KYBER1024	0.38	0.0012	0.0012	10,000

B. Tail Bound, DFR, and Sphere Packing

To gain more insight, we then estimate the magnitude of n_e based on (6). Without loss of generality, we let

$$n_e^{(\ell)} := [n_{e,1}, n_{e,2}, \dots, n_{e,\ell}]^T$$

to be the ℓ coefficients in n_e , where $1 \leq \ell \leq n$.

Lemma 2: $\Pr(\|n_e^{(\ell)}\| \leq z) \geq 1 - Q_{\ell/2} \left(\frac{\sqrt{\ell} \lceil q/2^{d_v+1} \rceil}{\sigma_G}, \frac{z}{\sigma_G} \right)$, where $Q_M(a, b)$ is the generalised Marcum Q-function.

Proof: See Appendix C. ■

Remark 2: With $\ell = 1$ and $z = \lfloor q/4 \rfloor$, we can easily show $\Pr(\|n_{e,1}\| \leq \lfloor q/4 \rfloor) \geq 1 - 2Q\left(\left(\lfloor q/4 \rfloor - \lceil q/2^{d_v+1} \rceil\right)/\sigma_G\right)$, where $Q(a)$ is the Q-function. It gives an explicit upper bound on the DFR of the original Kyber encoder in (5):

$$\delta \leq 1 - \left(1 - 2Q\left(\left(\lfloor q/4 \rfloor - \lceil q/2^{d_v+1} \rceil\right)/\sigma_G\right)\right)^n.$$

We have $\delta \leq 2^{-142}, 2^{-167}, 2^{-176}$, for KYBER512/768/1024, respectively. Note that δ is evaluated numerically in [3] [6].

Lemma 2 shows that Kyber decoding noise $n_e^{(\ell)}$ can be bounded with probability $1 - Q_{\ell/2}\left(\sqrt{\ell}\lceil q/2^{d_v+1} \rceil/\sigma_G, z/\sigma_G\right)$ by a hypersphere with radius z . Since the addition in (4) is over the modulo q domain, we can view the Kyber encoding problem as a sphere packing problem: an arrangement of non-overlapping spheres within a hypercube \mathbb{Z}_q^ℓ . The original Kyber uses the lattice codes $\lfloor q/2 \rfloor \mathbb{Z}_q^\ell$ for sphere packing purposes, which is far from optimal. Even for very small dimensions ℓ , there exist much denser lattices that maintain the same minimal distance between points. In the next section, we will construct lattice codes with denser packing and lower DFR.

IV. LATTICE CODES FOR KYBER

A. Lattice Codes, Hypercube Shaping, and CVP Decoding

Definition 1 (Lattice): An ℓ -dimensional lattice Λ is a discrete additive subgroup of \mathbb{R}^m , $m \leq \ell$. Based on ℓ linearly independent vectors b_1, \dots, b_ℓ in \mathbb{R}^m , Λ can be written as

$$\Lambda = \mathcal{L}(\mathbf{B}) = z_1 \mathbf{b}_1 + \dots + z_\ell \mathbf{b}_\ell,$$

where $z_1, \dots, z_\ell \in \mathbb{Z}$, and $\mathbf{B} = [\mathbf{b}_1, \dots, \mathbf{b}_\ell]$ is referred to as a generator matrix of Λ .

Definition 2 (Lattice Code): A lattice code $\mathcal{C}(\Lambda, \mathcal{P})$ is the finite set of points in Λ that lie within the region \mathcal{P} :

$$\mathcal{C}(\Lambda, \mathcal{P}) = \Lambda \cap \mathcal{P}.$$

If $\mathcal{P} = \mathbb{Z}_p^\ell$, then the lattice code $\mathcal{C}(\Lambda, \mathbb{Z}_p^\ell)$ is said to be generated from hypercube shaping (HS).

Definition 3 (CVP Decoder): Given an input $\mathbf{y} \in \mathbb{R}^\ell$, the Closest Vector Problem (CVP) decoder returns the closet lattice vector to \mathbf{y} over the lattice $\mathcal{L}(\mathbf{B})$, i.e.,

$$\mathbf{x} = \text{CVP}(\mathbf{y}, \mathcal{L}(\mathbf{B})) = \arg \min_{\mathbf{x}' \in \mathcal{L}(\mathbf{B})} \|\mathbf{x}' - \mathbf{y}\|.$$

Definition 4 (HS Encoder [5]): Considering the Smith Normal Form factorization (SNF) of a lattice basis \mathbf{B} , denoted as $\mathbf{B} = \mathbf{U} \cdot \text{diag}(\pi_1, \dots, \pi_\ell) \cdot \mathbf{U}'$, where $\mathbf{U}, \mathbf{U}' \in \mathbb{Z}^{\ell \times \ell}$ are unimodular matrices. Let the message space be

$$\mathcal{M}_{p,\ell} = \{0, 1, \dots, p/\pi_1 - 1\} \times \dots \times \{0, 1, \dots, p/\pi_\ell - 1\}. \quad (7)$$

where $p > 0$ is a common multiplier of π_1, \dots, π_ℓ . Given $\mathbf{m} \in \mathcal{M}_{p,\ell}$, a HS encoder returns a codeword $\mathbf{x} \in \mathcal{C}(\mathcal{L}(\mathbf{B}), \mathbb{Z}_p^\ell)$:

$$\mathbf{x} = \hat{\mathbf{B}} \mathbf{m} \pmod{p}, \quad (8)$$

where $\hat{\mathbf{B}} = \mathbf{U} \cdot \text{diag}(\pi_1, \dots, \pi_\ell)$.

Definition 5 (HS-CVP Decoder [5]): Let \mathbf{y} be a noisy version of $\mathbf{x} \in \mathcal{C}(\mathcal{L}(\mathbf{B}), \mathbb{Z}_p^\ell)$. The HS-CVP decoder returns an estimated message $\hat{\mathbf{m}} = [\hat{m}_1, \dots, \hat{m}_\ell]^T \in \mathcal{M}_{p,i}$:

$$\begin{aligned} \hat{\mathbf{m}} &= \text{HS-CVP}(\mathbf{y}, \mathcal{L}(\mathbf{B})) \\ &= \hat{\mathbf{B}}^{-1} \cdot \text{CVP}(\mathbf{y}, \mathcal{L}(\mathbf{B})) \pmod{(p/\pi_1, \dots, p/\pi_\ell)}, \quad (9) \end{aligned}$$

where $\hat{m}_i = (\hat{\mathbf{B}}^{-1} \text{CVP}(\mathbf{y}, \mathcal{L}(\mathbf{B})))_i \pmod{p/\pi_i}$, for $i = 1, \dots, \ell$.

For the choice of $\mathcal{L}(\mathbf{B})$, in this work, we consider Barnes–Wall lattice with $\ell = 16$ (BW16) and Leech lattice with

$\ell = 24$ (Leech24) [8]. They provide the optimal packing in the corresponding dimensional space and have fixed-complexity CVP decoders [5] [9]. Since the coefficients in Kyber are integers, we will scale the original generator matrix to an integer matrix $\mathbf{B} \in \mathbb{Z}^{\ell \times \ell}$, and use the corresponding $\hat{\mathbf{B}}$.

B. Lattice Encoder and Decoder for Kyber

We divide the n coefficients in m to $\kappa = n/\ell$ blocks:

$$m = [m_{\ell,1}, \dots, m_{\ell,\kappa}]^T,$$

where $m_{\ell,i} \in \mathcal{M}_{p,\ell}$ in (7) is the i^{th} block of coefficients in m , $i = 1, \dots, \kappa$. Consider the lattice encoder and decoder as described in Algorithms 4 and 5.

Algorithm 4 Λ -Enc(m): lattice encoder

//Replace Step 5 in Algorithm 2

- 1: $x_{\ell,i} := \hat{\mathbf{B}} \cdot m_{\ell,i} \pmod{p}$, $i = 1, \dots, \kappa$
 - 2: $x := [x_{\ell,1}, \dots, x_{\ell,\kappa}]^T$
 - 3: **return** $v := \text{Compress}_q(\mathbf{t}^T \mathbf{r} + e_2 + \lfloor q/p \rfloor \cdot x, d_v)$
-

Algorithm 5 Λ -Dec(\mathbf{u}, v): lattice decoder

//Replace Step 3 in Algorithm 3

- 1: $y := v - \mathbf{s}^T \cdot \mathbf{u} = [y_{\ell,1}, \dots, y_{\ell,\kappa}]^T$, where $y_{\ell,i}$ is the i^{th} block of coefficients in y
 - 2: $\hat{m}_{\ell,i} := \text{HS-CVP}(y_{\ell,i}/\lfloor q/p \rfloor, \mathcal{L}(\mathbf{B}))$, $i = 1, \dots, \kappa$
 - 3: **return** $\hat{m} := [\hat{m}_{\ell,1}, \dots, \hat{m}_{\ell,\kappa}]^T$
-

Remark 3: With $\mathcal{L}(\mathbf{B}) = \mathbb{Z}^\ell$, $\hat{\mathbf{B}} = I_\ell$, $p = 2$, the proposed encoder/decoder reduces to the original ones used in Kyber.

C. CER and DFR Reduction

The number of information bits for each block is given by

$$b(\ell, p) = \sum_{i=1}^{\ell} \log_2(p/\pi_i).$$

The total number of information bits is $\kappa b(\ell, p)$. As shown in Step 3 in Algorithm 4, the ciphertext size remains unchanged. For comparison purposes, we define the CER reduction ratio:

$$\text{CER-R} \triangleq 1 - n/\kappa b(\ell, p) = 1 - l/b(\ell, p).$$

Let $\lambda(p)$ be the length of a shortest non-zero vector in the lattice $\mathcal{L}(\lfloor q/p \rfloor \mathbf{B})$. The correct decoding radius of HS-CVP decoder is $\lambda(p)/2$. Let δ_i be the decryption failure rate for the i^{th} block of coefficients $\hat{m}_{\ell,i}$. Using Lemma 2, we have

$$\delta_i \leq Q_{\ell/2}\left(\sqrt{\ell}/\sigma_G \cdot \lceil q/2^{d_v+1} \rceil, \lambda(p)/(2\sigma_G)\right).$$

The decryption failure rate of κ blocks is given by

$$\delta = 1 - \prod_{i=1}^{\kappa} (1 - \delta_i) \approx \kappa Q_{\ell/2}\left(\sqrt{\ell}/\sigma_G \cdot \lceil q/2^{d_v+1} \rceil, \lambda(p)/(2\sigma_G)\right).$$

Table III compares the normalized correct decoding radius $\lambda(p)/(2 \lfloor q/2 \rfloor)$, CER reduction, and δ for difference lattices.

TABLE III
LATTICE CODES FOR KYBER

	$\mathbb{Z}^\ell : p = 2$ [6]	BW16 : $p = 4$	Leech24 : $p = 8$
$r(p)/(2 \lfloor q/2 \rfloor)$	0.5	0.7067	0.7067
$b(\ell, p)/\ell$	1	20/16	36/24
Plaintext size	256	320	380*
CER-R	0%	20%	32.6%
δ : KYBER512	2^{-139}	2^{-149}	2^{-111}
δ : KYBER768	2^{-164}	2^{-177}	2^{-131}
δ : KYBER1024	2^{-174}	2^{-259}	2^{-226}

*: Since $256 = 10 \times 24 + 16$, we consider 10 Leech24 codewords with $p = 8$ and 1 BW16 codeword with $p = 4$.

D. Decoding Complexity, Security, and Observation

As shown in (9), the decoding complexity is determined by the CVP decoder for the selected lattice. For BW16 lattice, the running time of CVP decoder is proportional to 32ℓ [5]. For Leech lattice, the CVP decoder requires 3595 real operations in the worst case [9]. Since lattice encoder/decoding doesn't affect the M-LWE hardness assumption in Kyber [6], the security arguments remain the same.

We observe a tradeoff between CER and DFR from Table III: a smaller CER requires a larger p , which will reduce the correct decoding radius of $\mathcal{L}(\lfloor q/p \rfloor \mathbf{B})$ accordingly. Interestingly, KYBER1024 enjoys a much lower DFR compared to KYBER512/768. This can be explained by the smallest noise variance shown in Table II. This work focuses on reducing CER with a fixed ciphertext size. Our future work includes reducing CER given a fixed plaintext size, e.g., 256 bits.

APPENDIX

A. Proof of Theorem 1

According to Lemma 1, with $n = 256$, the distribution of $\mathbf{e}^T \mathbf{r}$ in (2) is well-approximated as a multivariate normal distribution, i.e., $\mathbf{e}^T \mathbf{r} \leftarrow \mathcal{N}(0, kn\eta_1^2/4 \cdot I_n)$. Since $e_2 \leftarrow \beta\eta_2$ behaves very similarly to a (discrete) Gaussian with variance $\eta_2/2$, the distribution of $\mathbf{e}^T \mathbf{r} + e_2$ is well-approximated by

$$\mathbf{e}^T \mathbf{r} + e_2 \leftarrow \mathcal{N}(0, (kn\eta_1^2/4 + \eta_2/2)I_n). \quad (10)$$

We then estimate the distribution of $\mathbf{s}^T (\mathbf{e}_1 + \mathbf{c}_u)$. According to [6], the distribution of $\mathbf{e}_1 + \mathbf{c}_u$ behaves very similarly to a Gaussian with the same variance $\eta_2/2 + \text{Var}(\psi_{d_u})$, i.e.,

$$\mathbf{e}_1 + \mathbf{c}_u \leftarrow \mathcal{N}(0, (\eta_2/2 + \text{Var}(\psi_{d_u}))I_n). \quad (11)$$

Using Remark 1, the distribution of $\mathbf{s}^T (\mathbf{e}_1 + \mathbf{c}_u)$ is well-approximated as

$$\mathbf{s}^T (\mathbf{e}_1 + \mathbf{c}_u) \leftarrow \mathcal{N}(0, (kn\eta_1/2 \cdot (\eta_2/2 + \text{Var}(\psi_{d_u})))I_n). \quad (12)$$

Given (10), (12), and (3), for a large n , we can obtain (6).

B. Proof of Lemma 1

The proof is similar to that given in [7, Theorem 3]. Let $Y = ZZ'$, we have that Y has components $Y_i = \sum_{j=0}^{n-1} \xi(i-j)Z_{i-j}Z'_j$, where $\xi(x) = \text{sign}(x)$ for $x \neq 0$ and $\xi(0) = 1$ [10, p. 338]. Note that $Z_{i-j} = Z_{(i-j) \bmod n}$. The mean of such a component Y_i is given by

$$E(Y_i) = \sum_{j=0}^{n-1} E(\xi(i-j)Z_{i-j}Z'_j) = 0.$$

The summands of a component Y_i are independent, so the variance is given by

$$\text{Var}(Y_i) = \sum_{j=0}^{n-1} \text{Var}(\xi(i-j)Z_{i-j}Z'_j) = n/4 \cdot \eta\eta'. \quad (13)$$

A similar argument shows that covariance of distinct components Y_i and $Y_{i'}$ for $i \neq i'$ is given by

$$\begin{aligned} & \text{Cov}(Y_i, Y_{i'}) \\ &= E\left(\sum_{j=0}^{n-1} \xi(i-j)Z_{i-j}Z'_j \cdot \sum_{j'=0}^{n-1} \xi(i'-j')Z_{i'-j'}Z'_{j'}\right) \\ & \quad - \sum_{j=0}^{n-1} E(\xi(i-j)Z_{i-j}Z'_j) \sum_{j'=0}^{n-1} E(\xi(i'-j')Z_{i'-j'}Z'_{j'}) \\ &= (\eta'/2) \cdot \sum_{j=0}^{n-1} \xi(i-j)\xi(i'-j)E(Z_{i-j})E(Z_{i'-j}) \\ & \quad + (\eta/2) \cdot \sum_{t=0}^{n-1} E(Z'_{i-t})E(Z'_{i'-t}) \\ &= 0. \end{aligned} \quad (14)$$

Furthermore, the summands of Y_i are independent and identically distributed, so a Central Limit argument shows that the

distribution of Y_i is well-approximated by a normal distribution for large n . Thus Y can be approximated by a multivariate normal distribution. So we have $Y \leftarrow \mathcal{N}(0, n/4 \cdot \eta\eta' I_n)$.

C. Proof of Lemma 2

Given Theorem 1, we can write $n_{e,i} = x_i + y_i$, where $x_i \leftarrow \mathcal{N}(0, \sigma_G^2)$ and $y_i \leftarrow \mathcal{U}(-\lceil q/2^{d_v+1} \rceil, \lceil q/2^{d_v+1} \rceil)$. Let $\mathbf{y} = [y_1, y_2, \dots, y_\ell]^T$ and $N_U = 2\lceil q/2^{d_v+1} \rceil + 1$. We have

$$\begin{aligned} & \Pr\left(\|\mathbf{n}_e^{(\ell)}\| \leq z\right) \\ &= \Pr\left(\sqrt{\sum_{i=1}^{\ell} (x_i + y_i)^2} \leq z\right) \\ &= \sum_{j=1}^{N_U^\ell} \Pr\left(\sqrt{\sum_{i=1}^{\ell} (x_i + \mu_{j,i})^2} \leq z \mid \mathbf{y} = \mu_j\right) \Pr(\mathbf{y} = \mu_j) \\ &= \frac{1}{N_U^\ell} \sum_{j=1}^{N_U^\ell} \Pr\left(\sqrt{\sum_{i=1}^{\ell} (x_i + \mu_{j,i})^2} \leq z \mid \mathbf{y} = \mu_j\right), \end{aligned}$$

where $\mu_j = [\mu_{j,1}, \mu_{j,2}, \dots, \mu_{j,\ell}]^T$ is a sample point in the sample space of \mathbf{y} . Given $y_i = \mu_{j,i}$, $\sqrt{\sum_{i=1}^{\ell} (x_i + \mu_{j,i})^2}$ follows non-central chi distribution, i.e.,

$$\begin{aligned} & \Pr\left(\sqrt{\sum_{i=1}^{\ell} (x_i + \mu_{j,i})^2} / \sigma_G \leq z / \sigma_G \mid \mathbf{y}_j = \mu_j\right) \\ &= 1 - Q_{\ell/2}\left(\sqrt{\sum_{i=1}^{\ell} \mu_{j,i}^2} / \sigma_G, z / \sigma_G\right), \end{aligned}$$

where $Q_M(a, b)$ is the generalized Marcum Q-function. Since $Q_M(a, b)$ is strictly increasing in a for all $a \geq 0$, we have

$$\begin{aligned} \Pr\left(\|\mathbf{n}_e^{(\ell)}\| \leq z\right) &= 1 - \frac{1}{N_U^\ell} \sum_{j=1}^{N_U^\ell} Q_{\ell/2}\left(\sqrt{\sum_{i=1}^{\ell} \mu_{j,i}^2} / \sigma_G, z / \sigma_G\right) \\ &\geq 1 - Q_{\ell/2}\left(\sqrt{\ell} / \sigma_G \cdot \lceil q/2^{d_v+1} \rceil, z / \sigma_G\right). \end{aligned}$$

REFERENCES

- [1] The NIST PQC Team, "PQC standardization process: Announcing four candidates to be standardized, plus fourth round candidates," 2022. [Online]. Available: <https://csrc.nist.gov/News/2022/pqc-candidates-to-be-standardized-and-round-4>
- [2] National Institute of Standards and Technology, "Module-Lattice-based Key Encapsulation Mechanism Standard," *Federal Information Processing Standards Publication (FIPS) NIST FIPS 203 ipd.*, 2023. [Online]. Available: <https://doi.org/10.6028/NIST.FIPS.203.ipd>
- [3] J. Bos, L. Ducas, E. Kiltz, T. Lepoint, V. Lyubashevsky, J. M. Schanck, P. Schwabe, G. Seiler, and D. Stehlé, "CRYSTALS - Kyber: A CCA-Secure Module-Lattice-Based KEM," in *2018 IEEE European Symposium on Security and Privacy (EuroS&P)*, 2018, pp. 353–367.
- [4] I. Papadopoulos and J. Wang, "Polar codes for Module-LWE public key encryption: The case of Kyber," *Cryptography*, vol. 7, no. 1, 2023. [Online]. Available: <https://www.mdpi.com/2410-387X/7/1/2>
- [5] S. Lyu, L. Liu, C. Ling, J. Lai, and H. Chen, "Lattice codes for lattice-based PKE," *Cryptology ePrint Archive, Paper 2022/874*, 2022. [Online]. Available: <https://eprint.iacr.org/2022/874>
- [6] R. Avanzi, J. Bos, L. Ducas, E. Kiltz, T. Lepoint, V. Lyubashevsky, J. Schanck, P. Schwabe, G. Seiler, and D. Stehlé, "Algorithm specifications and supporting documentation (version 3.02)," *Tech. rep., Submission to the NIST post-quantum project (2021)*, 2021. [Online]. Available: <https://pq-crystals.org/kyber/resources.shtml>
- [7] A. Costache, B. R. Curtis, E. Hales, S. Murphy, T. Ogilvie, and R. Player, "On the precision loss in approximate homomorphic encryption," *Cryptology ePrint Archive, Paper 2022/162*, 2022. [Online]. Available: <https://eprint.iacr.org/2022/162>
- [8] J. H. Conway and N. J. A. Sloane, *Sphere Packings, Lattices, and Groups*, 2nd ed. New York: Springer-Verlag, 1993.
- [9] A. Vardy and Y. Be'ery, "Maximum likelihood decoding of the Leech lattice," *IEEE Transactions on Information Theory*, vol. 39, no. 4, pp. 1435–1444, 1993.
- [10] X. Ding, M. F. Esgin, A. Sakzad, and R. Steinfeld, "An injectivity analysis of Crystals-Kyber and implications on quantum security," in *Information Security and Privacy*. Cham: Springer International Publishing, 2022, pp. 332–351.